

A predictive sliding mode control for quadrotor's tracking trajectory subject to wind gusts and uncertainties

Dounia Meradi¹, Zoubir Abdeslem Benselama¹, Ramdane Hedjar²

¹Department of Electronics, Saad Dahlab University, Blida, Algeria

²Department of Computer Engineering, King Saud University, Riyadh, Saudi Arabia

Article Info

Article history:

Received Jul 27, 2021

Revised May 28, 2022

Accepted Jun 12, 2022

Keywords:

Discrete-time sliding mode control

Non-linear model predictive control

Predictive sliding mode control

Quadrotor

Wind gusts

ABSTRACT

In this paper, a predictive sliding mode control (PSMC) strategy for the quadrotors tracking trajectory problem is proposed. This strategy aims to combine the advantages of sliding mode control (SMC) and non-linear model predictive control (NMPC) to improve the tracking control performance for quadrotors in terms of optimality, inputs/states constraints satisfaction, and strong robustness against disturbances. A comparative study of three popular controllers: the SMC, NMPC, and the integral backstepping control (IBC) is performed with different criteria. Accordingly, IBC and SMC show less computational time and strong robustness, while NMPC has minimum control effort. The discrete Dryden turbulence model is used as a benchmark model to represent the wind effect on the trajectory tracking accuracy. The effectiveness of the proposed method PSMC has been proven and compared with discrete-time sliding mode control (DSMC) and NMPC in several scenarios. Simulation results show that under both wind turbulence and time-variant uncertainties, the PSMC outperforms the other controllers by providing simultaneously disturbance rejection and guarantee that the control inputs are within bounded constraints.

This is an open access article under the [CC BY-SA](https://creativecommons.org/licenses/by-sa/4.0/) license.



Corresponding Author:

Dounia Meradi

Department of Electronics, Signal Processing and Image Laboratory, Saad Dahlab University

Blida 1, BP 270, Route de soumaa, Ouled Yaïch, Blida, Algeria

Email: dounia.meradi@g.enp.edu.dz

1. INTRODUCTION

With the technological advancements in the field of unmanned aerial vehicles (UAVs), the quadrotor has aroused particular interest in vertical take-off and landing vehicles (VTOL) and has become a popular research platform for testing numerous control techniques. Unlike the conventional helicopters and due to its small size, payload capability, simple mechanical structure, and smooth maneuverability, the quadrotor is allowed to fly in indoor or outdoor environments, as well as near obstacles. Because of the numerous physical phenomena that affect the quadrotor dynamics such as the aerodynamic effect, the gravity center, and the gyroscopes effects. Thus, the quadrotor can be considered among the most complex flying systems. Consequently, the exact modeling of the quadrotor is required in order to design a suitable flight controller. There are various ways of expressing the motion dynamics, which mainly depend on the rotation parametrization. The most common attitude parametrizations are: Euler angles, axis-angle, rotation matrix [1], Rodrigues parameters [2], and unit quaternion [3]. Euler angles are widely used to present the quadrotor's orientation, it is simple, unique, and can be easily understood. It suffers however from gimbal lock phenomena.

The proportional integral derivative (PID), linear quadratic regulator (LQR), H_∞ [4], and gain schedul-

ing [5] are the common linear controllers used to command the quad-rotors due to their simplicity. However, they can guarantee the closed-loop stability only around an equilibrium point. Besides, they usually fail to track aggressive maneuvers. Several non-linear controls have been developed to conquer some of the shortcomings and limitations of linear control. Among them, fuzzy logic controller [6], adaptive sliding mode control (SMC) [7], [8], and neural networks (NN) [9], [10].

The SMC has been significantly used to control the quad-rotor. Because of its attractive finite-time convergence characteristics and robustness to parametric uncertainties and perturbations. Since the SMC suffers from the chattering phenomena caused by the reaching law and has high control effort, many researchers have been working on those troubles. One of the proposed solutions is the integral sliding mode control [11]. The integral action added to the sliding manifold has the ability to eliminate the reaching phase and reduce the chattering on the control inputs. Ahmad *et al.* [12] applied an improved integral power rate exponential reaching law (IIPRERL) sliding mode control strategy to deal with the unwanted chattering problem, stability, and the oscillations in the quadrotor responses in the presence of matched disturbances. The simulation results of IIPRERL-SMC have shown no chattering on the control inputs compared to SMC. In discrete-time, the authors in [13] have proposed the discrete-time sliding mode control (DSMC) for quadrotor where the linear extrapolation method has been employed to obtain the discrete-time model of the quadrotor.

In the realm of optimal control for quadrotor, both of the linear and non-linear model predictive control (MPC) has been widely used, showing a good tracking ability, handling to input/state constraints [14] and avoiding obstacles [15]. In [16], a nonlinear and linear MPC have been presented for a quadrotor to track different references trajectories where the non-linear model predictive control (NMPC) has been made by using a state-dependent coefficient representation. Moreover, stability analysis of Unconstrained/constrained for both controllers has been provided. The simulation results in the case of with or without disturbances showed that the NMPC outperformed the linear MPC. Since the MPC depends explicitly on accurate model-plant as well as that the quadrotor is a strongly constrained coupled non-linear system which is usually prone to parameters variation on mass and inertia due to payload. For that, any mismatched parameters or disturbances can decrease the stability of the system when using the conventional MPC approaches.

Many researchers have been combined the SMC and MPC. In [17], the surface parameters of sliding mode control have been determined and updated using the non-linear model predictive control. In [18], the sliding mode predictive control has been used to control the boiler-turbine system deal with uncertainties and system constraints. The adopted control strategy was based on the dual-mode law that is constructed of two-part: the discrete sliding mode control law where the sliding surface was in the terminal sliding region, and the receding horizon optimization law where the sliding surface was out from the terminal sliding region. A comparative study between DSMC with predictive sliding function (PSF) and predictive sliding mode control is done in [19]. Those strategies are simulated to the linearised isothermal Van de Vussen systems. The simulation results have shown that both of the combination controllers have outperformed the NMPC and SMC. As well as, the DSMC with PSF has more ability to eliminate the chattering compared to the PSMC. While this latter has strong robustness to disturbances.

Upon to the aforementioned discussion and motivated by those works [18], [20], [21], the main contribution of this paper can be encapsulated in the following: i) a discrete sliding mode control is proposed to control the quadrotor with the calculation of the desired orientation, ii) design an NMPC with the multiple-shooting concept in order to accelerate and improve the convergence of the optimization control problem (OCP), and iii) an insensitivity to external disturbances, a robustness to parametric uncertainties, a state/inputs constraints satisfaction and optimal control are undertaking and ensuring simultaneously by the proposed PSMC.

The roadmap for the remainder of the paper has been organized in the following way: subsection 2.1 develops the quadrotor's dynamic model and its discrete-time formulation. Subection 2.2 seeks to design the control law strategy of DSMC, then NMPC, and in the end the PSMC. Simulation results with different scenarios are shown in section 3 and finally, the conclusion is in section 4.

2. METHOD

2.1. Quadrotor's model dynamic

The quadrotor is a VTOL vehicle able to perform quasi-stationary flights. It consists of four fixed-pitch blades coupled with DC brush-less motors fixed to the end of a rigid cross-shaped body as shown in Figure 1. Indeed, each propeller is rotating at a certain angular speed ω_i generates a force F_i and a moment M_i

that are given by:

$$F_i = b\omega_i^2, M_i = d\omega_i^2$$

with $i = 1 : 4$, and b, d are the thrust and drag coefficients, respectively.

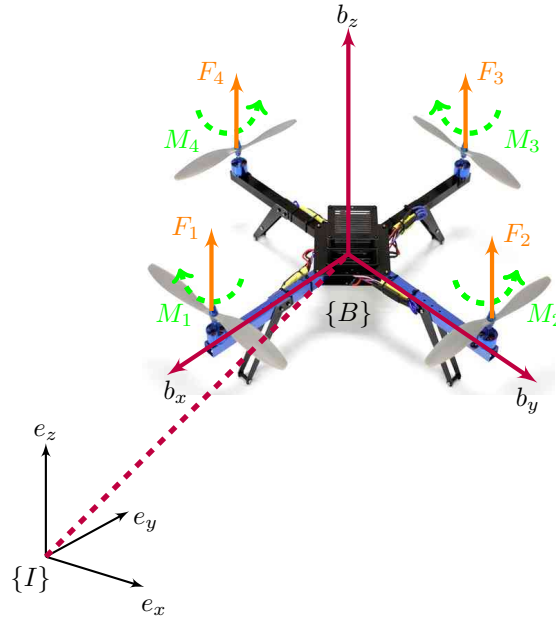


Figure 1. The coordinate system frames

To describe the mathematical model of the quadrotor, we define two reference coordinate frames represented in Figure 1. The inertial frame $\{I\}$ is defined by $\{e_x, e_y, e_z\}$, and the body-fixed frame $\{B\}$ attached to the quadrotor's gravity center and is defined by $\{b_x, b_y, b_z\}$. To describe the quadrotor's rotation, we use Z-Y-X convention of Euler angles $\{\phi, \theta, \psi\}$. Therefore, the attitude of the quadrotor is represented by the rotation matrix R which allows the passage from frame $\{B\}$ to frame $\{I\}$ and is defined [22]:

$$R = \begin{bmatrix} c_\theta c_\psi & -c_\phi s_\psi + s_\phi s_\theta c_\psi & s_\phi s_\psi + c_\phi s_\theta c_\psi \\ c_\theta s_\psi & c_\phi c_\psi + s_\phi s_\theta s_\psi & -s_\phi c_\psi + c_\phi s_\theta s_\psi \\ -s_\theta & s_\phi c_\theta & c_\phi c_\theta \end{bmatrix} \quad (1)$$

where c_x (resp. s_x) represents the simplified notation of $\cos(x)$ (resp. $\sin(x)$).

By applying the fundamental principle of dynamics, we obtain the equations representing the dynamic behaviour of the quadrotor:

$$\begin{cases} m\ddot{r} = RTe_z + mge_z + K_{ft}v + F_{des} \\ J\dot{\Omega} = -\Omega^\times J\Omega + \tau + \tau_{des} \end{cases} \quad (2)$$

where $r = [x, y, z]^T$ represents the position of the quadrotor, $\Omega = [\Omega_x, \Omega_y, \Omega_z]$ is the body angular velocity, $m, I = \text{diag}(I_x, I_y, I_z)$ are the total mass of the quadrotor and moments of inertia respectively, $T = \sum_{i=1}^4 b\omega_i$, $\tau = [\tau_x, \tau_y, \tau_z]^T$ represent the thrust force expressed in B -frame and the aerodynamic moments generated by the propellers respectively. The terms $F_{des}, \tau_{des} \in \mathbb{R}^3$ represent the external disturbances applied on the quadrotor. Finally, The terms $K_{ft} = \text{diag}(K_{ft_x}, K_{ft_y}, K_{ft_z})$ denote the translation drag coefficients and $(x)^\times$ represents the skew-matrix of the vector x .

The relation between the derivative of Euler angles and the body angular velocities is expressed as (3):

$$\begin{bmatrix} \Omega_x \\ \Omega_y \\ \Omega_z \end{bmatrix} = \begin{bmatrix} 1 & 0 & -s_\theta \\ 0 & c_\theta & s_\phi c_\theta \\ 0 & s_\theta & c_\phi c_\theta \end{bmatrix} \times \begin{bmatrix} \dot{\phi} \\ \dot{\theta} \\ \dot{\psi} \end{bmatrix} \quad (3)$$

The relation between the propellers angular speeds and the generated aerodynamic forces and the moments due to the propellers is expressed as (4):

$$\begin{bmatrix} u_1 \\ u_2 \\ u_3 \\ u_4 \end{bmatrix} = \begin{bmatrix} b & b & b & b \\ 0 & -lb & 0 & lb \\ -lb & 0 & lb & 0 \\ d & -d & d & -d \end{bmatrix} \times \begin{bmatrix} \omega_1^2 \\ \omega_2^2 \\ \omega_3^2 \\ \omega_4^2 \end{bmatrix} \quad (4)$$

From (2), the quadrotor is an under-actuated system with four inputs $\{T, \tau_x, \tau_y, \tau_z\}$ and six outputs $\{x, y, z, \phi, \theta, \psi\}$. To put the quadrotor equations in state-space form, the state vector of the system $x \in \mathbb{R}^{12}$ is chosen as (5):

$$\begin{aligned} x &= [x, \dot{x}, y, \dot{y}, z, \dot{z}, \phi, \dot{\phi}, \theta, \dot{\theta}, \psi, \dot{\psi}]^T \\ &= [x_1, x_2, x_3, x_4, x_5, x_6, x_7, x_8, x_9, x_{10}, x_{11}, x_{12}]^T \end{aligned} \quad (5)$$

The physical limitations of the quadrotor's motors speeds are bounded between minimum angular velocity ω and maximum angular velocity $\bar{\omega}$. The maximum and minimum of thrust force and torques values providing by these limitations are:

$$\begin{aligned} 4b\omega^2 &\leq u_1 \leq 4b\bar{\omega}^2 \\ bl(\omega^2 - \bar{\omega}^2) &\leq u_2 \leq bl(\bar{\omega}^2 - \omega^2) \\ bl(\omega^2 - \bar{\omega}^2) &\leq u_3 \leq bl(\bar{\omega}^2 - \omega^2) \\ 2d(\omega^2 - \bar{\omega}^2) &\leq u_4 \leq 2d(\bar{\omega}^2 - \omega^2) \end{aligned} \quad (6)$$

where $[u_1, u_2, u_3, u_4]^T = [T, \tau_x, \tau_y, \tau_z]^T$ for simple notification.

2.1.1. Discrete time quadrotor's model

According to (2) and (5) the dynamic model can be written in compact form:

$$\dot{x}(t) := \begin{cases} x_{2i-1}(t) = x_{2i}(t), & i = 1, 2, \dots, 6 \\ x_{2i}(t) = f_i(x(t)) + \Delta f_i(x(t)) + (g_i(x(t)) + \Delta g_i(x(t)))u(t) + w_i(t) \end{cases} \quad (7)$$

Using forward Euler discretization, we obtain the discrete system of (7) as in (8):

$$x[k] := \begin{cases} x_{2i-1}[k+1] = x_{2i-1}[k] + hx_{2i}[k] & i = 1, 2, \dots, 6 \\ x_{2i}[k+1] = x_{2i}[k] + h(f_i(x[k]) + \Delta f_i(x[k]) + (g_i(x[k]) + \Delta g_i(x[k]))u[k]) + w_i[k] \end{cases} \quad (8)$$

where h is sampling time, k represents the k -th sampling time, $f_i(x[k])$ and $g_i(x[k])$ are given in Appendix. $\Delta f_i(\cdot)$ and $\Delta g_i(\cdot)$ denote the bounded unknown parametric uncertainties, $w_i[k]$ is the bounded external disturbance, where: $\Delta f_i(\cdot) \leq \Delta f_{i_{max}}$, $\Delta g_i(\cdot) \leq \Delta g_{i_{max}}$ and $w_i[k] \leq w_{i_{max}}$.

The discrete dynamic system in (8) can be rewritten as (9):

$$\begin{cases} x_{2i-1}[k+1] = x_{2i-1}[k] + hx_{2i}[k], & i = 1, 2, \dots, 6 \\ x_{2i}[k+1] = x_{2i}[k] + h(f_i(x[k]) + g_i(x[k])u[k]) + d[k] \end{cases} \quad (9)$$

where $d[k] = h(\Delta f_i(x[k]) + \Delta g_i(x[k])u[k]) + w_i[k]$. Let $u[k] = [u_1[k], u_2[k], u_3[k], u_4[k]]^T$ being the control input. The main objective is to synthesize a non-linear control laws for a quad-rotor in order to track the desired trajectory $\{x_d, y_d, z_d, \psi_d\}$. In the next section, we assume the case without disturbances, i.e $d[k] = 0$ and it is unknown to the controllers.

2.2. Control design

In this subsection, we synthesis and describe the different non-linear control laws that have been used in this paper for the trajectory tracking of the quad-rotor. First, we start the synthesis of the discrete sliding mode control DSMC. Then, the non-linear model predictive control principle is presented. Finally, the combined sliding mode with predictive control PSCM is designed.

2.2.1. Design of discrete sliding mode control approach

The objective of the SMC law is to constrain the system state trajectory (9) to be reached and then to maintain it on the sliding surface even in the presence of uncertainties in the system. Let a second-order Slotine surface [23] is chosen as (10):

$$s_i[k] = e_{2i}[k] + \lambda_i e_{2i-1}[k], \quad i = 1, 2, \dots, 6 \quad (10)$$

where the $\lambda_i \in R^+$ are the constants of tuning, $e[k]$ are the tracking error which is the difference between the actual state $x[k]$ and the desired one $r[k]$ and is defined:

$$e[k] = \begin{cases} e_{2i-1}[k] = r_{2i-1}[k] - x_{2i-1}[k] \\ e_{2i}[k] = r_{2i}[k] - x_{2i}[k] \end{cases} \quad (11)$$

where $r[k]$ is the discrete-time of the desired trajectory $r(t) = [x_d, \dot{x}_d, y_d, \dot{y}_d, z_d, \dot{z}_d, \phi_d, \dot{\phi}_d, \theta_d, \dot{\theta}_d, \psi_d, \dot{\psi}_d]$. $\{x_d, y_d, z_d, \psi_d\}$ and its derivatives are provided from the trajectory generator, while $\{\phi_d, \theta_d\}$ and its derivative can be deduced from the position controller.

The purpose of the control is to force the system to evolve on the sliding surface and prevent it from getting out of it,

$$S = \{e[k] \mid s_i(e[k]) = 0, i = 1, 2, \dots, 6\} \quad (12)$$

We introduce the virtual command $v_i[k]$ in such a way that $x_{2i}[k+1] = v_i[k]$, which gives us:

$$v_i[k] = x_{2i}[k] + h(f_i(x[k]) + g_i(x[k])u[k]) \quad (13)$$

The dynamic of the surface (10) is:

$$\begin{aligned} s_i[k+1] &= s_i[k] + e_{2i}[k+1] + \lambda_i e_{2i-1}[k+1] \\ &= s_i[k] + (r_{2i}[k+1] - v_i[k]) + \lambda_i e_{2i-1}[k+1] \end{aligned} \quad (14)$$

The Gao's reaching dynamics of the sliding surface are [24]:

$$s_i[k+1] = (1 - h\sigma_i) s_i[k] - h\mu_i \text{sign}(s_i[k]), \quad i = 1, 2, \dots, 6 \quad (15)$$

where σ_i and μ_i are tuning parameters and satisfying $0 \leq h\sigma_i < 1$ and $\mu_i > 0$.

By equating (15) and (14), the following virtual commands signal are obtained:

$$\begin{aligned} v_i[k] &= \sigma_i s_i[k] + \mu_i \text{sign}(s_i[k]) + \lambda_i e_{2i-1}[k+1] + r_{2i}[k+1], \\ & \quad i = 1, 2, \dots, 6 \end{aligned} \quad (16)$$

By applying the properties of the rotation matrix [25], we determine the real commands:

$$\begin{aligned} u_1[k] &= m \sqrt{(V_1[k])^2 + (V_2[k])^2 + (V_3[k])^2} \\ u_2[k] &= \frac{V_4[k]}{g_4([x_k])}, u_3[k] = \frac{V_5[k]}{g_5([x_k])}, u_4[k] = \frac{V_6[k]}{g_6([x_k])} \end{aligned} \quad (17)$$

where $V_i[k] = v_i[k] - f_i(x[k])$, $i = 1, 2, \dots, 6$.

The desired roll and pitch angles ϕ_d and θ_d are generated from:

$$\begin{cases} m(V_1[k]c_{\psi} + V_2[k]s_{\psi}) = s_{\theta}u_1[k] \\ m(V_1[k]s_{\psi} + V_2[k]c_{\psi}) = s_{\phi}c_{\theta}u_1[k] \\ mV_3[k] = c_{\phi}c_{\theta}u_1[k] \end{cases} \quad (18)$$

We draw from (18):

$$\begin{cases} \phi_d = \arctan\left(\frac{V_1[k]s_{\psi_d} - V_2[k]c_{\psi_d}}{V_3[k]}\right) \\ \theta_d = \arctan\left(\frac{V_1[k]c_{\psi_d} + V_2[k]s_{\psi_d}}{\sqrt{(V_1[k]s_{\psi_d} - V_2[k]c_{\psi_d})^2 + V_3[k]^2}}\right) \end{cases} \quad (19)$$

To alleviate the chattering problem caused by the discontinuous sign function. We replace this latter by a pseudo-sign function which is defined:

$$psign(x, \eta) = \frac{x}{|x| + \eta} \quad (20)$$

where $0 < \eta \ll 1$ has been chosen equal to 0.05.

2.2.2. Design of non-linear model predictive control NMPC

The predictive control problem consists of determining the control vector u that minimizes the selected cost function while ensuring the satisfaction of the constraints. It can be summarized as the following steps:

- At each sampling time k , the future system outputs are predicted over a prediction horizon N using the preceding inputs and outputs. These predictions are noted $x[k + j|k]$, $j = 0, 1, \dots, N$ to indicate the value of the output at instant $k + j$, calculated at the instant k
- The sequence of future commands $u[k + j|k]$, $j = 0, 1, \dots, N - 1$ is calculated by optimizing a certain determined criterion so that the predicted output $x[k + j|k]$ is as close as possible to the reference trajectory $r[k + j|k]$, $j = 1, \dots, N$, while minimizing the control effort
- Finally, Only the first component $u[k|k]$ of the optimal control sequence $u[k|k + j]$ is applied to the system. At the next sampling time $k + 1$, the resolution begins again with step one by taking into account the new updated measurements of the system $x[k + 1]$ and a new control sequence $u[k + 1|k + 1 + j]$, $j = 0, \dots, N - 1$ is determined. The control sequence is improved at each sampling period since new measurements could be taken and consequently the vector of the control signal $u[k + 1|k + 1 + j]$, $j = 0, 1, \dots, N - 1$ will be in principle different from $u[k + j|k]$, $j = 0, 1, \dots, N$.

Based on the above definition, the discrete-time NMPC formulation with multiple shooting is:

$$\min_{u[k+j|k], x[k+j|k]} \sum_{k=0}^{N-1} L_r(x[k], u[k], r[k]) + L_t(x[N]) \quad (21a)$$

$$\mathbf{s.t.} : x[0] - x_0 = 0 \quad (21b)$$

$$x[k + 1] - x[k] - f_{RK4}(x[k], u[k]) = 0, \quad j = 0, \dots, N \quad (21c)$$

$$x[k] \in \mathcal{X}, \quad k = 0, \dots, N \quad (21d)$$

$$u[k] \in \mathcal{U}, \quad k = 0, \dots, N - 1 \quad (21e)$$

where (21d) and (21e) are respectively, the sets of constraint on states (map margins and Euler-angles limitations $-\frac{\pi}{2} < \phi < \frac{\pi}{2}$, $-\frac{\pi}{2} < \theta < \frac{\pi}{2}$, $-\pi < \psi < \pi$) and on inputs that were defined in (6). x_0 is the current state. The running cost function denotes $L_r(x[k], u[k], r[j])$ and is equal to:

$$L_r(x[k], u[k], r[k]) = \|r[k] - x[k]\|_Q^2 + \|u_{ref}[k] - u[k]\|_R^2 \tag{22}$$

and $L_t(x[N])$ being the terminal cost function and is equal to: $L(x[N]) = \|r[N] - x[N]\|_H^2$. Where $Q, H \in \mathbb{R}^{12 \times 12}$, $R \in \mathbb{R}^{4 \times 4}$ are a positive-definite tuning matrix.

The control input reference u_{ref} is taken to obtain better tracking performance based on desired trajectory acceleration and defined as: $u_{ref} = [m\sqrt{a_1^2 + a_2^2 + (a_3 + g)^2}, 0, 0, 0]^T$. Where a_1, a_2 and a_3 are the discrete time of desired trajectory acceleration $\{\ddot{x}_d, \ddot{y}_d, \ddot{z}_d\}$.

Herein (21c), the concept of direct multiple shooting [26] is defined as an equality constraint, where $f_{RK4}(\cdot)$ is the Runge Kutta 4th integration and is defined as (23):

$$\begin{aligned} k_1 &= f(x[k], u[k]) \\ k_2 &= f(x[k] + \frac{h}{2}k_1, u[k]) \\ k_3 &= f(x[k] + \frac{h}{2}k_2, u[k]) \\ k_4 &= f(x[k] + hk_3, u[k]) \\ f_{RK4}(x[k], u[k]) &= 1/6(k_1 + 2k_2 + 2k_3 + k_4) \end{aligned} \tag{23}$$

and, $f(x[k], u[k]) = [x_{2i}, f_i(x[k]) + g_i(x[k])u[k]]^T, i = 1, \dots, 6$.

2.2.3. Non-linear predictive sliding mode control

The non-linear predictive sliding mode control (PSMC) control law is used in this work for the quadrotor trajectory tracking problems. This hybrid approach is based on the NMPC and the DSMC in order to provide the best trade-off between minimum effort energy control, tracking trajectory, and rejection of disturbance. The main objective of PSMC is to generate the optimum control input where the PSMC concept is illustrated in Figure 2. Firstly, at each sampling time k , the DSMC part calculates the reference sliding surfaces $s_{ref}[k + j|k], j = 0, \dots, N$ over the horizon N , invoking the (10) and (15) yields:

$$\begin{aligned} s_{ref}[k] &= s[k] \\ s_{ref}[k + 1] &= (1 - h\sigma)s_{ref}[k] - h\mu s_{ref}[k] \\ s_{ref}[k + N] &= (1 - h\sigma)s_{ref}[k + N - 1] - h\mu s_{ref}[k + N - 1] \end{aligned} \tag{24}$$

Then, the NMPC computes the control sequence $u[k|k + j]$ using the plant-model. The computations optimize the tracking of the predicted sliding functions $s_{pred}[k + j|k], j = 0, \dots, N$ while minimizing the control effort. In the end, the first element of the calculated control sequence is applied to the quadrotor model Figure 2.

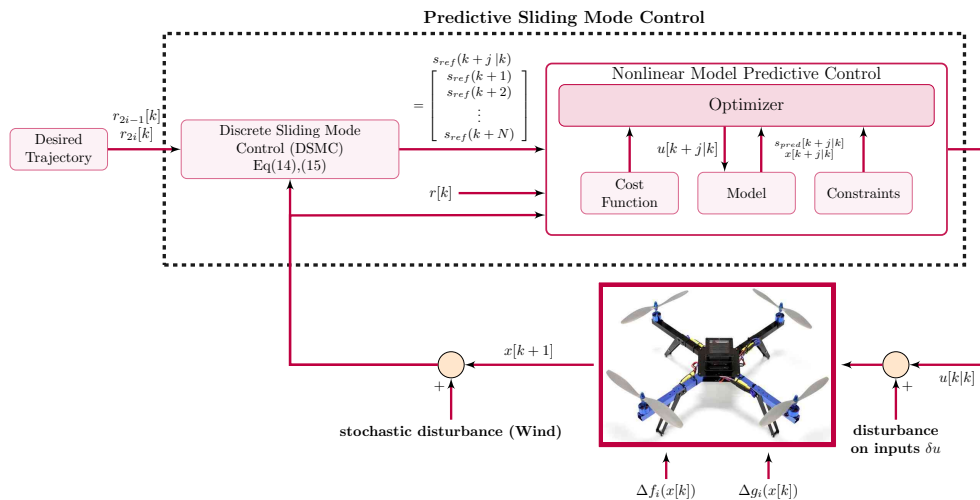


Figure 2. Block diagram of predictive sliding mode control strategy

The mathematical formulation of the non-linear PSMC can be written:

$$\min_{u[k+j|k], x[k+j|k], s[k+j|k]} \sum_{k=0}^{N-1} J_r(x, s, u, r) + J_t(x[N], s[N]) \quad (25a)$$

$$\mathbf{s.t.} : x[0] - x_0 = 0, \quad (25b)$$

$$x[k+1] = x[k] + hf(x[k], u[k]) \quad (25c)$$

$$s_{pred_i}[k+1] = s_{pred_i}[k] + e_{2i}[k+1] + \lambda_i e_{2i-1}[k+1] \quad (25d)$$

$$x[k] \in \mathcal{X}, \quad k = 0, \dots, N \quad (25e)$$

$$u[k] \in \mathcal{U}, \quad k = 0, \dots, N-1 \quad (25f)$$

$$s_{pred}[k] \in \mathcal{S}, \quad k = 0, \dots, N \quad (25g)$$

where $J_r(\cdot)$ is the running cost function of PSMC and is defined as (26):

$$J_r(x, s, u, r) = \|u_{ref}[k] - u[k]\|_R^2 + \|s_{pred}[k] - s_{ref}[k]\|_\lambda^2 \quad (26)$$

and, $J_t(\cdot) = \|s_{pred}[N] - s_{ref}[N]\|_\eta^2$ is the terminal cost function, $\lambda, \eta \in \mathbb{R}^{6 \times 6}$ are a positive-definite tuning matrix which penalize the tracking surface functions. \mathcal{X}, \mathcal{U} are the same specified in 2.2.2, \mathcal{S} is the set of terminal sliding region that is defined as [21], [24]:

$$\mathcal{S} = \bigcup_{i=1}^6 \mathcal{S}_i, \quad \mathcal{S}_i = \{x \mid |s_i(x)| \leq \Delta_i, x \in \mathcal{X}, u \in \mathcal{U}, \Delta_i = h\mu_i\} \quad (27)$$

3. SIMULATION RESULTS AND DISCUSSION

Simulation results using MATLAB/Simulink are developed in this section to corroborate the proposed controllers' effectiveness. The quadrotor dynamic model from (2) is used to perform all simulations. The sampling period of the simulation is set to $h = 10 \text{ ms}$, and the initial conditions are set to zero except in the case 3.1. The quadrotor and controllers parameters are given in Tables 1 and 2, respectively. The OCP in (21) and (25) are transformed into a nonlinear programming problem (NLP) and simulated using CasADi toolkit [27]. Furthermore, an interior point optimizer (IPOPT) is used to solve the NLP, using up to 2,000 iterations, a tolerance of 10^{-6} , and the horizon prediction N set to 15. In addition, the constraints on inputs, states and sliding mode band are tacking:

$$\mathcal{X} := \begin{cases} x_1 \in]-\infty, +\infty[\\ \vdots \\ x_6 \in]-\infty, +\infty[\\ x_7 \in \left[-\frac{\pi}{2}, \frac{\pi}{2}\right] \\ x_8 \in]-\infty, +\infty[\\ x_9 \in \left[-\frac{\pi}{2}, \frac{\pi}{2}\right] \\ x_{10} \in]-\infty, +\infty[\\ x_{11} \in [-\pi, \pi] \\ x_{12} \in]-\infty, +\infty[\end{cases}, \quad \mathcal{U} := \begin{cases} u_1 \in [0, 9.3585] \\ u_2 \in [-0.5849, 0.5849] \\ u_3 \in [-0.5849, 0.5849] \\ u_4 \in [-0.0507, 0.0507] \end{cases}, \quad (28)$$

$$\mathcal{S} := \begin{cases} |s_i[k+1]| < \frac{h\mu_i}{1-h\sigma_i} \\ i = 1, \dots, 6. \end{cases}$$

With the aim of carrying out a comparative study between the SMC, integral backstepping control (IBC), and NMPC controllers, the following performance indexes are taken into account:

- The control signal energy (CSE) and the control effort energy (CEE):

$$CSE = \sum_{k=1}^n u^2[k], \quad CEE = \sum_{k=1}^n (u[k] - u[k-1])^2 \quad (29)$$

- The average computational time.
- The position root mean square error (PRMSE)

$$PRMSE(cm) = \sqrt{\frac{\sum_{k=1}^n \left((x_d[k] - x[k])^2 + (y_d[k] - y[k])^2 + (z_d[k] - z[k])^2 \right)}{n}} \quad (30)$$

- The attitude root mean square error (ARMSE)

$$ARMSE(^{\circ}) = \sqrt{\frac{\sum_{k=1}^n \left((\phi_d[k] - \phi[k])^2 + (\theta_d[k] - \theta[k])^2 + (\psi_d[k] - \psi[k])^2 \right)}{n}} \quad (31)$$

Table 1. Quadrotor's parameters

Symbol	Value	Unit
m	0.486	kg
g	9.806	m/s ²
l	0.25	m
b	2.9842×10^{-5}	N/rad/s
d	3.232×10^{-7}	N.m/rad/s
I	$\begin{pmatrix} 3.8278 & 0 & 0 \\ 0 & 3.8288 & 0 \\ 0 & 0 & 7.6566 \end{pmatrix} \times 10^{-3}$	kg/m ²
K_{ft}	$\begin{pmatrix} 5.567 & 0 & 0 \\ 0 & 5.567 & 0 \\ 0 & 0 & 6.354 \end{pmatrix} \times 10^{-4}$	N/m/s
ω	0	rad/s
$\bar{\omega}$	280	rad/s

Results of the comparative study of the three commands are shown in Table 3. The IBC and SMC have been developed in [28]. Moreover, the disturbances, wind turbulence, and uncertainties used in this case are the same in the aforementioned paper. Regarding the criteria that indicates the amount of energy consumed by the controllers, it can be seen that the smallest CSE values with respect to u_1 , u_2 , u_3 , and u_4 is determined based on the NMPC approach for both cases (with or without disturbances) compared to SMC and IBC. Besides, NMPC provides the lowest fluctuations and smoothness at control inputs which are revealed by the CEE values. Nevertheless, the NMPC shows a high computational burden compared to other controllers. As a result of the chattering phenomena, the SMC approach has a high effort (CEE and CSE values) compared to the other controllers. For the three controllers without disturbances, it can be noticed that the PRMSE and ARMSE values are less than 0.06 cm and 0.09 deg respectively which are considered tolerable. While, in the presence of disturbances, the SMC outperforms the IBC and NMPC showing good tracking ability in terms of ARMSE and PRMSE. To demonstrate the effectiveness of the PSMC control, this latter compared to the NMPC and DSMC controls with the following different scenarios.

3.1. Case 1: nominal performance comparison

The simulation is done here performed using nominal conditions, to track an inclined 8-shaped trajectory without any considering disturbances or parametric uncertainties, and with an initial condition different from the equilibrium point. Simulation results in this case are presented in Figure 3 from Figures 3(a) to 3(i). As can be shown in Figures 3(a)-3(d) and 3(i), all controllers achieve successful tracking. In contrast, the DSMC and PSMC exhibit a response time faster than NMPC. The control efforts are shown in the Figures 3(e)-3(h). While in Figures 3(g) and 3(h), the DSMC has a large control effort exceeding the control limits for the pitch and yaw torques in comparison with PSMC and NMPC.

Table 2. Controllers' parameters

Controller	Symbol	Value
DSMC	λ_i	71 71 18.5 10 10 25
	μ_i	7.9 7.9 0.9 1.9 1.9 6.9
	σ_i	0.02 0.02 0.18 0.2 0.2 0.5
NMPC	Q	$diag([0.5, .05, .5, .05, 60, 20, 20, 3, 20, 3, 65, 53.5])$
	H	$10 \times Q$
	R	$diag([1, 10^{-2}, 10^{-2}, 10^{-3}])$
PSMC	R	$diag([1, 10^{-2}, 10^{-2}, 10^{-3}])$
	λ_i	0.05 0.05 18.5 10 10 11
	μ	$diag([0.85, 0.85, 0.005, 0.22, 0.22, 0.35])$
	σ	$diag([1, 1, 1.5, 0.55, 0.55, 1.85])$

Table 3. A comparison between SMC, IBC, and NMPC tracking of straight-line trajectory. It is done with CSE and CEE of $\{u_1, u_2, u_3, u_4\}^T$, Average time, PRMSE, and ARMS criteria

	Controller	CSE	CEE	Average Time [ms]	PRMSE [cm]	ARMSE [deg]
without disturbances	IBC	4.5407e+04	2.2729e-04	0.8528	0.0051	0.0718
		0.0021	8.9765e-05			
		0.0069	2.3942e-04			
	SMC	4.7647e-04	5.6564e-08	0.6636	0.0151	0.0459
		4.5407e+04	2.3160e-04			
		0.0074	9.2390e-04			
		0.0457	0.0022			
		5.2894e-04	5.7366e-08			
		4.5407e+04	2.1768e-04			
	NMPC	4.4816e-04	1.4897e-05	16	0.0584	0.0047
		5.7965e-04	1.5780e-05			
		4.7172e-04	5.5041e-08			
with disturbances	IBC	6.0236e+04	2.9813	1.6	0.8133	1.9414
		13.2886	1.1165			
		8.1007	0.6525			
	SMC	3.3047	0.0016	1.5	0.1470	0.4943
		6.0241e+04	7.9003			
		30.8017	5.1253			
		21.1184	3.8687			
		3.3084	0.0021			
		6.0191e+04	0.2527			
	NMPC	0.8102	9.6626e-04	26.7	4.6709	1.6334
		0.8088	0.0010			
		3.2275	0.0008			

3.2. Case 2: wind gusts rejection ability

In this case, the quadrotor is undergoing sudden wind gusts as external disturbances in the interval [10, 30] s. The Dryden wind turbulence model [29] is used to generate a stochastic velocities disturbance added to the dynamics of the quadrotor, as shown in Figure 4. This has had a great influence on the dynamics of the aircraft, in particular, the linear, and angular velocities. Figures 4(a) and 4(b) illustrate respectively the linear and angular velocity components of the applied wind turbulence. Figure 5 from Figures 5(a) to 5(i) depict the quadrotor response to track the square trajectory against wind gusts effect with the three controllers. The NMPC fails to track the reference trajectory in the presence of wind, in particular in X and Y positions Figures 5(a) and 5(b) which has a large error that reaches 0.4 m. With the outperforming of DSMC, this latter and PSMC exhibit strong tracking ability against wind gusts. As for the control effort, the NMPC has a minimum effort even in the presence of wind Figures 5(e)-5(h). Although, the DSMC's good tracking, it has a large control effort; more chattering phenomena and exceeds the control limits Figures 5(f) and 5(g). While, the PSMC control effort remains within a limits control, and has minimum chattering compared to DSMC. On the other hand, the DSMC shows some interesting robustness properties, but in the presence of saturation on inputs, the stability cannot be ensured. Figures 5(a) to 5(d) shows how the quadrotor deviates when it is controlled via the DSMC with saturation on inputs represented by a blue dash-dotted line. Figure 5(i) shows 3D tracking square trajectory, both of PSMC and DSMC are successfully tracking the desired trajectory even in the wind presence, while the NMPC cannot follow the desired trajectory and deviate from it.

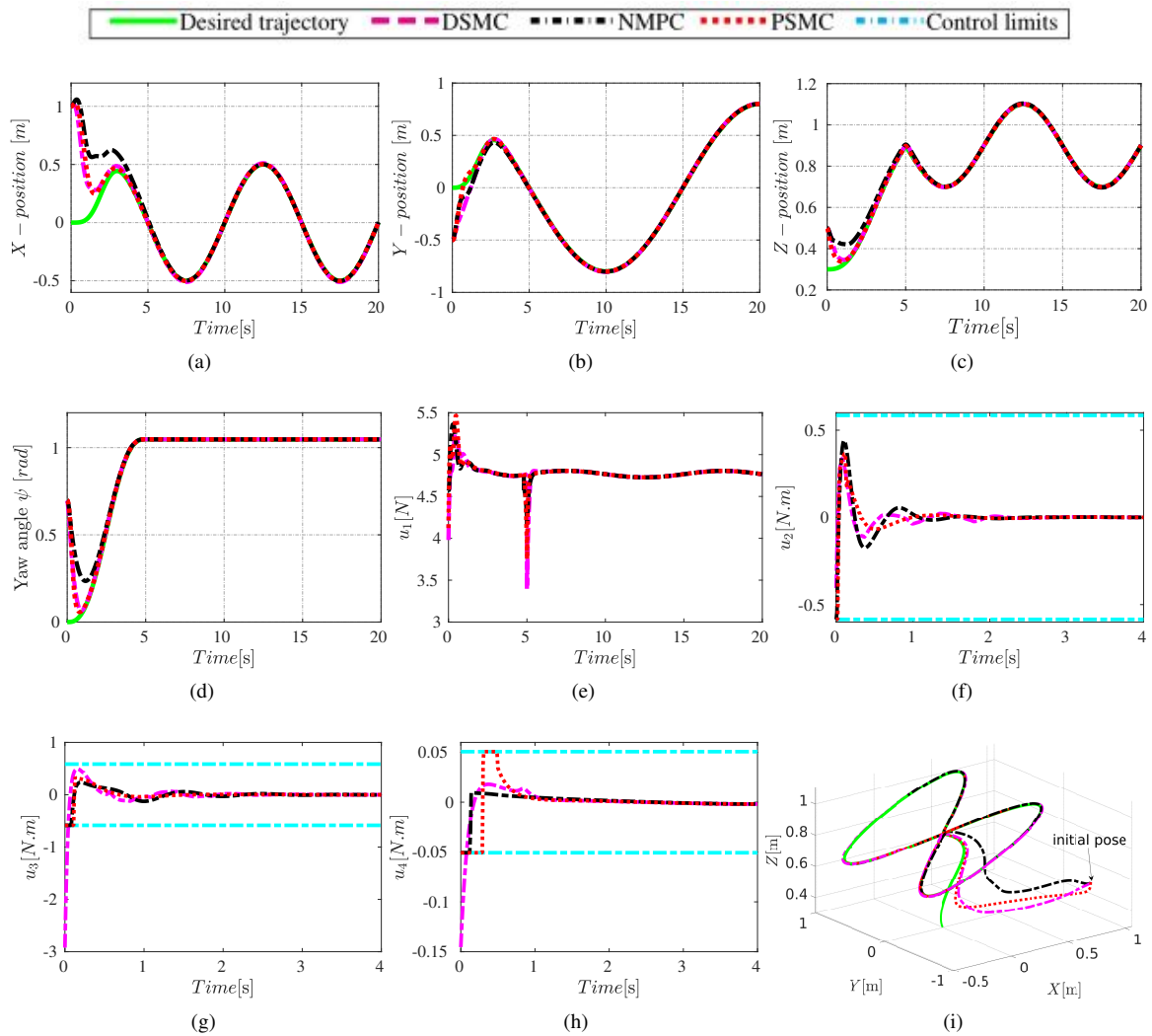


Figure 3. The results of tracking an inclined 8-shaped trajectory in nominal condition with initial condition $x_0 = [-15^\circ, 0, 35^\circ, 0, 40^\circ, 0, 1, 0, -0.5, 0, 0.5, 0]^T$: (a)-(d) the tracking trajectory, (e)-(h) the control inputs, (i) the 3-D tracking trajectory

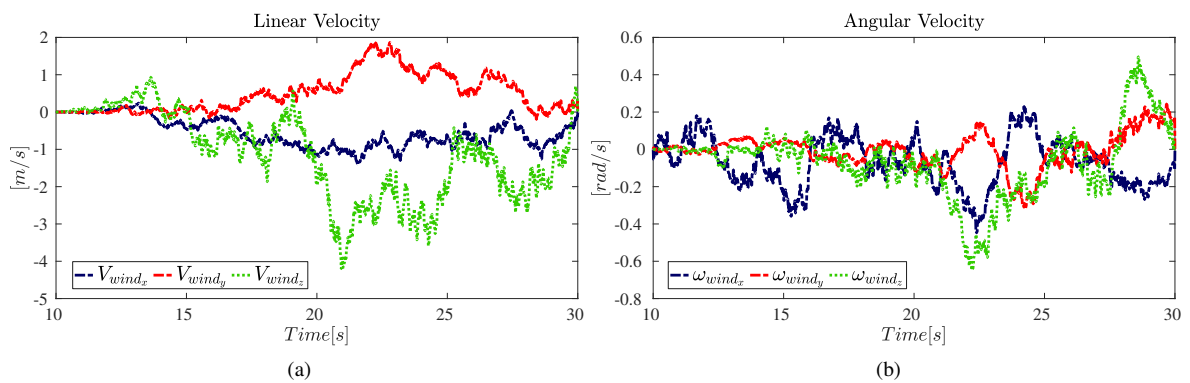


Figure 4. Velocity components of the applied wind turbulence in the interval [10, 30]s: (a) the linear V_{wind} and (b) angular ω_{wind}

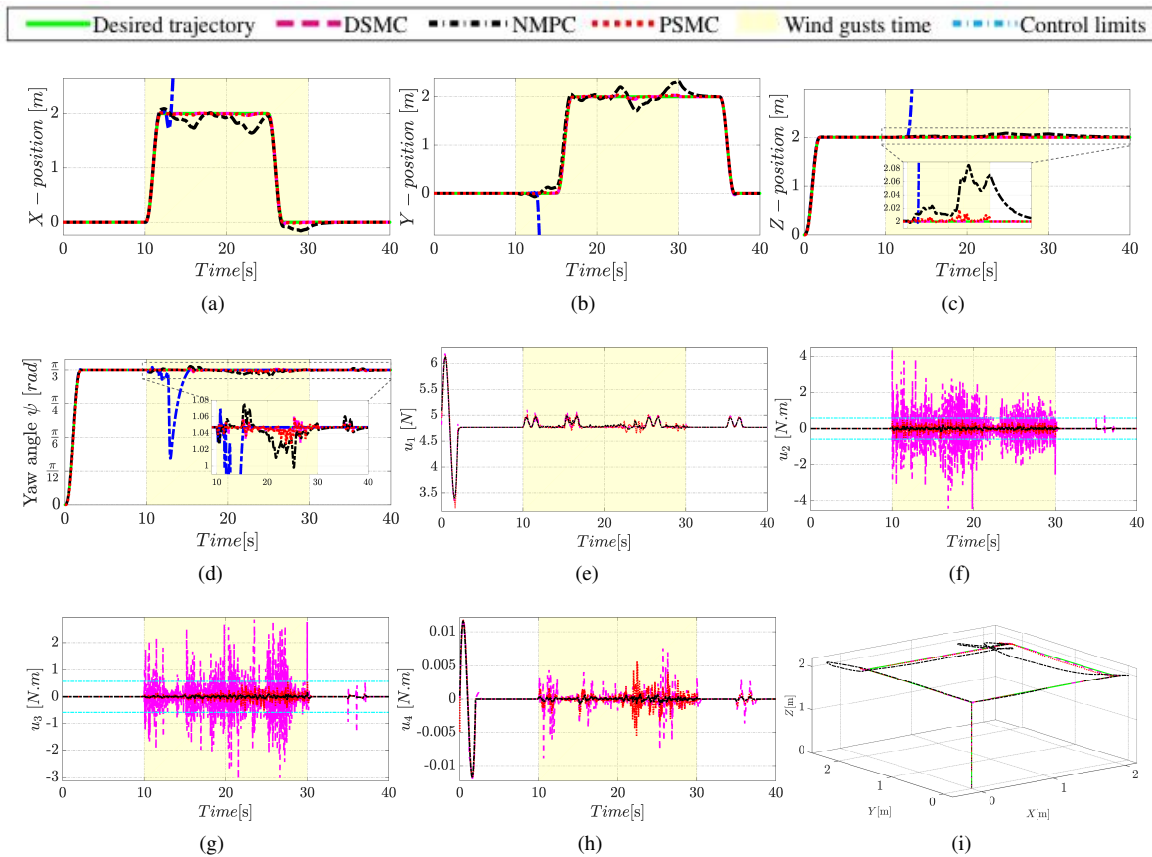


Figure 5. Simulation results showing tracking of square references under wind turbulence in the interval 10,30 s: (a)-(d) tracking trajectory, (e)-(h) the control inputs, and (i) 3-D tracking trajectory. The marked area indicates the turbulence wind period, and the blue dash-dotted line indicates the DSMC with saturation on inputs

3.3. Case 3: robustness comparison in the presence of model mismatch

In this case, to check the controllers’ robustness, the unmodeled dynamics are included in the mathematical model of the quadrotor. Since the mass m and the inertia matrix $I = \text{diag}(I_x, I_y, I_z)$ are time-variant in the first at interval 10-30 s, 40% variations of these parameters which are unknown to the controllers, and they are assumed:

$$\tilde{m} = m (1 + 0.4 \sin(0.5t) + \gamma)$$

$$\tilde{I} = I_3 \times (1 + 0.4 \sin(0.5t)) I$$

where $\gamma = -0.125 + 0.25 \times \text{rand}(1)$ and $\text{rand}(\cdot)$ is a MATLAB function that generates a random number between 0 and 1, and I_3 is (3×3) identity matrix.

In the second period 40-50 s, we assume that there are uncertainties on the drag and thrust coefficients which are ordinarily difficult to identify. From (4), this variations on d and b parameters induce a disturbances on the control inputs as follow: $\tilde{u} = u + \delta u$, where δu is the added disturbances caused by mismatches thrust and drag coefficients on the control inputs and is equal to $\delta u = [2, 0.5, 0.5, 0.05]^T$.

Figure 6 shows the response of the nonlinear controllers under uncertainties. As it can be seen the PSMC preserves its good tracking performance with small tracking errors Figures 6(a) to 6(d). In Figures 6(e) to 6(h), it’s observed that DSMC inputs exceeds the limitations on control inputs and has more chattering compared to PSMC in the presence of mismatched mass and inertia, while NMPC and PSMC preserve the control inputs within bounded constraints.

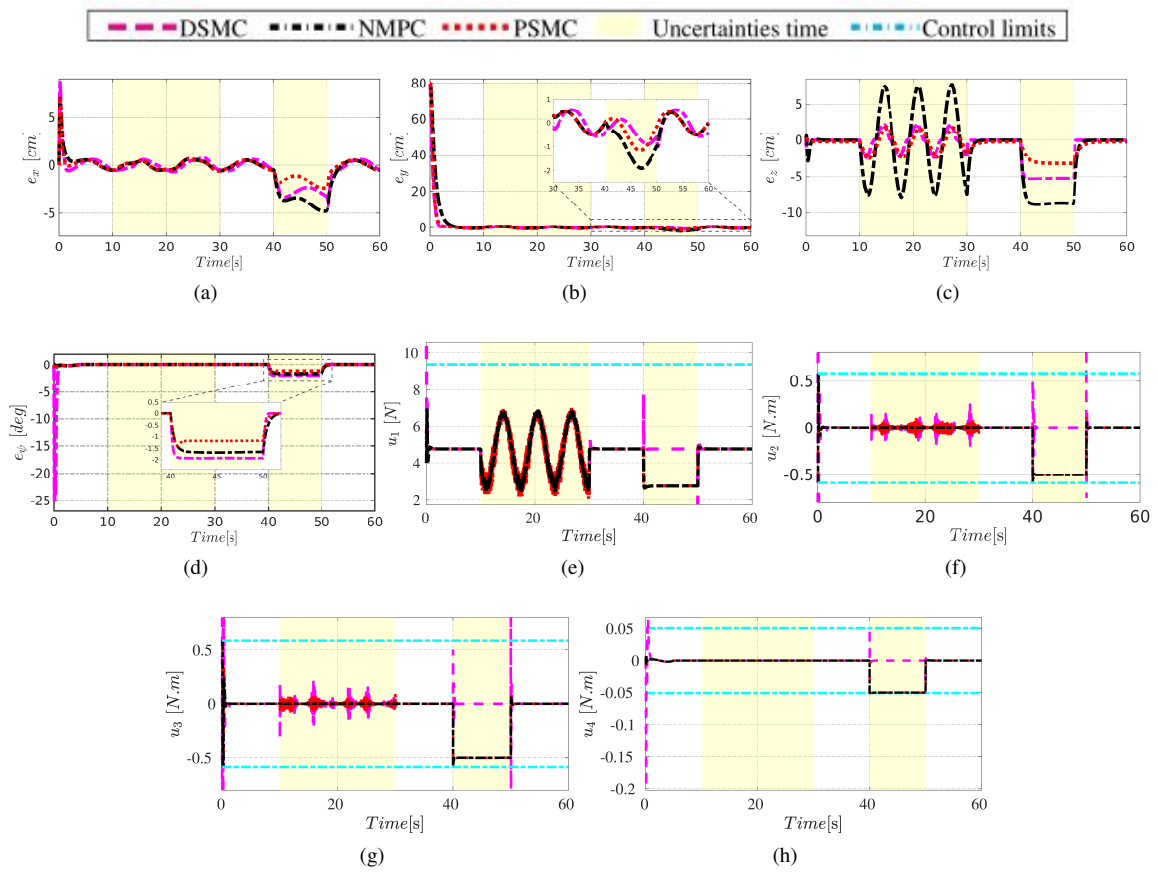


Figure 6. Control performance under parameters uncertainties with helix trajectory (a)-(d) tracking trajectory error and (e)-(h) the control inputs

4. CONCLUSION

In this paper, the PSMC control strategy is proposed to ensure simultaneously the inputs constraint and robustness with regard to sudden stochastic disturbances (wind turbulence), and time-variant parametric uncertainties. This work elaborated from a comparative study between different nonlinear control approaches. The controllers NMPC, IBC, and SMC have been tested in simulation. The SMC controller exhibited the robustness against disturbances, while the NMPC has shown lower control effort. These results conduct us to propose PSMC that merges DSMC and NMPC advantages. The simulation results shown the outperformed performances of the proposed PSMC with regards to NMPC, IBC, and SMC. Future works comprise the incorporation of the adaptive mechanism with PSMC for parameters uncertainties problem to enhance tracking accuracy in presence of unmodeled dynamics. Further, stability and feasibility analysis will be investigated by including a nonlinear observer of the state.

APPENDIX

$$\begin{aligned}
 f_1(x[k]) &= \frac{K_{ftx}}{m} x_1[k], & f_4(x[k]) &= \frac{(I_y - I_z)}{I_x} x_{10}[k] x_{12}[k], \\
 f_2(x[k]) &= \frac{K_{fty}}{m} x_3[k], & f_5(x[k]) &= \frac{(I_z - I_x)}{I_y} x_8[k] x_{12}[k], \\
 f_3(x[k]) &= \frac{K_{ftz}}{m} x_5[k] - g, & f_6(x[k]) &= \frac{(I_x - I_y)}{I_z} x_8[k] x_{10}[k].
 \end{aligned} \tag{32}$$

$$\begin{aligned}
 g_1(x[k]) &= \frac{1}{m} (\cos(x_1[k]) \cos(x_5[k]) \sin(x_3[k]) + \sin(x_1[k]) \sin(x_5[k])), & g_4(x[k]) &= \frac{l}{I_x}, \\
 g_2(x[k]) &= \frac{1}{m} (\cos(x_1[k]) \sin(x_3[k]) \sin(x_5[k]) - \sin(x_1[k]) \cos(x_5[k])), & g_5(x[k]) &= \frac{l}{I_y}, \\
 g_3(x[k]) &= \frac{1}{m} \cos(x_1[k]) \cos(x_3[k]), & g_6(x[k]) &= \frac{1}{I_z}.
 \end{aligned} \tag{33}$$





REFERENCES

- [1] A. H. Ginting, O. Wahyunggoro, and A. I. Cahyadi, "Attitude control of quadrotor using PD plus feedforward controller on SO(3)," *International Journal of Electrical and Computer Engineering (IJECE)*, vol. 8, no. 1, pp. 566–575, Feb. 2018, doi: 10.11591/ijece.v8i1.pp566-575.
- [2] B. E. Jackson, K. Tracy, and Z. Manchester, "Planning with attitude," *IEEE Robotics and Automation Letters*, vol. 6, no. 3, pp. 5658–5664, Jul. 2021, doi: 10.1109/LRA.2021.3052431.
- [3] J. Pliego-Jiménez, "Quaternion-based adaptive control for trajectory tracking of quadrotor unmanned aerial vehicles," *International Journal of Adaptive Control and Signal Processing*, vol. 35, no. 5, pp. 628–641, May 2021, doi: 10.1002/acs.3218.
- [4] H. Wang, Z. Li, H. Xiong, and X. Nian "Robust H_∞ attitude tracking control of a quadrotor uav on so (3) via variation-based linearization and interval matrix approach," *ISA Transactions*, vol. 87, pp. 10–16, Apr. 2019, doi: 10.1016/j.isatra.2018.11.015.
- [5] A. Ataka *et al.*, "Controllability and observability analysis of the gain scheduling based linearization for UAV quadrotor," in *2013 International Conference on Robotics, Biomimetics, Intelligent Computational Systems*, Nov. 2013, pp. 212–218, doi: 10.1109/ROBIONETICS.2013.6743606.
- [6] A. Al-Mahturi, F. Santoso, M. A. Garratt, and S. G. Anavatti, "Modeling and control of a quadrotor unmanned aerial vehicle using type-2 fuzzy systems," in *Unmanned Aerial Systems*, Elsevier, 2021, pp. 25–46, doi: 10.1016/B978-0-12-820276-0.00009-1.
- [7] M. Labbadi and M. Cherkaoui, "Robust adaptive global time-varying sliding-mode control for finite-time tracker design of quadrotor drone subjected to gaussian random parametric uncertainties and disturbances," *International Journal of Control, Automation and Systems*, vol. 19, no. 6, pp. 2213–2223, Jun. 2021, doi: 10.1007/s12555-020-0329-5.
- [8] X. Shi *et al.*, "Adaptive fractional-order SMC controller design for unmanned quadrotor helicopter under actuator fault and disturbances," *IEEE Access*, vol. 8, pp. 103792–103802, 2020, doi: 10.1109/ACCESS.2020.2998698.
- [9] M. Bisheban and T. Lee, "Geometric adaptive control with neural networks for a quadrotor in wind fields," *IEEE Transactions on Control Systems Technology*, vol. 29, no. 4, pp. 1533–1548, Jul. 2021, doi: 10.1109/TCST.2020.3006184.
- [10] K. Liu, R. Wang, X. Wang, and X. Wang, "Anti-saturation adaptive finite-time neural network based fault-tolerant tracking control for a quadrotor UAV with external disturbances," *Aerospace Science and Technology*, vol. 115, Aug. 2021, doi: 10.1016/j.ast.2021.106790.
- [11] B. Mu, K. Zhang, and Y. Shi, "Integral sliding mode flight controller design for a quadrotor and the application in a heterogeneous multi-agent system," *IEEE Transactions on Industrial Electronics*, vol. 64, no. 12, pp. 9389–9398, Dec. 2017, doi: 10.1109/TIE.2017.2711575.
- [12] I. Ahmad, M. Liaquat, F. M. Malik, H. Ullah, and U. Ali, "Variants of the sliding mode control in presence of external disturbance for quadrotor," *IEEE Access*, vol. 8, pp. 227810–227824, 2020, doi: 10.1109/ACCESS.2020.3041678.
- [13] J.-J. Xiong and G. Zhang, "Discrete-time sliding mode control for a quadrotor UAV," *Optik*, vol. 127, no. 8, pp. 3718–3722, Apr. 2016, doi: 10.1016/j.ijleo.2016.01.010.
- [14] N. T. Nguyen, I. Prodan, and L. Lefevre, "Multi-layer optimization-based control design for quadcopter trajectory tracking," in *2017 25th Mediterranean Conference on Control and Automation (MED)*, Jul. 2017, pp. 601–606, doi: 10.1109/MED.2017.7984183.
- [15] G. Garimella, M. Sheckells, and M. Kobilarov, "Robust obstacle avoidance for aerial platforms using adaptive model predictive control," in *2017 IEEE International Conference on Robotics and Automation (ICRA)*, May 2017, pp. 5876–5882, doi: 10.1109/ICRA.2017.7989692.
- [16] P. Ru and K. Subbarao, "Nonlinear model predictive control for unmanned aerial vehicles," *Aerospace*, vol. 4, no. 2, Jun. 2017, doi: 10.3390/aerospace4020031.
- [17] L. C. McNinch and H. Ashrafiuon, "Predictive and sliding mode cascade control for unmanned surface vessels," in *Proceedings of the 2011 American Control Conference*, Jun. 2011, pp. 184–189, doi: 10.1109/ACC.2011.5991049.
- [18] Z. Tian, J. Yuan, X. Zhang, L. Kong, and J. Wang, "Modeling and sliding mode predictive control of the ultra-supercritical boiler-turbine system with uncertainties and input constraints," *ISA Transactions*, vol. 76, pp. 43–56, May. 2018, doi: 10.1016/j.isatra.2018.03.004.





- [19] H. B. Mansour, K. Dehri, and A. S. Nouri, "Comparison between predictive sliding mode control and sliding mode control with predictive sliding function," in *International Conference on Electrical Engineering and Control Applications*, 2017, vol. 411, pp. 80–97, doi: 10.1007/978-3-319-48929-2_7.
- [20] A. Musa, L. R. Sabug, and A. Monti, "Robust predictive sliding mode control for multiterminal HVDC grids," *IEEE Transactions on Power Delivery*, vol. 33, no. 4, pp. 1545–1555, Aug. 2018, doi: 10.1109/TPWRD.2018.2811560.
- [21] J. Zhou, Z. Liu, and R. Pei, "A new nonlinear model predictive control scheme for discrete-time system based on sliding mode control," in *Proceedings of the 2001 American Control Conference*, 2001, pp. 3079–3084, doi: 10.1109/ACC.2001.946390.
- [22] K. J. Waldron and J. Schmiedeler, "Kinematics," in *Springer Handbook of Robotics*, B. Siciliano and O. Khatib, Eds. Cham: Springer International Publishing, 2016, pp. 11–36, doi: 10.1007/978-3-319-32552-1_2.
- [23] J. J. E. Slotine and W. Li, *Applied nonlinear control*, vol. 199, no. 1. New Jersey: Prentice Hall, 1991.
- [24] W. Gao, Y. Wang, and A. Homaifa, "Discrete-time variable structure control systems," *IEEE Transactions on Industrial Electronics*, vol. 42, no. 2, pp. 117–122, 1995, doi: 10.1109/41.370376.
- [25] G. Costa and G. Fogli, "The rotation group," in *Formalized Mathematics*, vol. 20, no. 1, 2012, pp. 27–41, doi: 10.1007/978-3-642-15482-9_2.
- [26] C. Kirches, "The direct multiple shooting method for optimal control," in *Fast Numerical Methods for Mixed-Integer Nonlinear Model-Predictive Control*, Wiesbaden: Springer, 2011, pp. 13–29., doi: 10.1007/978-3-8348-8202-8_2.
- [27] J. A. E. Andersson, J. Gillis, G. Horn, J. B. Rawlings, and M. Diehl, "CasADi: a software framework for nonlinear optimization and optimal control," *Mathematical Programming Computation*, vol. 11, no. 1, pp. 1–36, Mar. 2019, doi: 10.1007/s12532-018-0139-4.
- [28] M. Dounia, B. Z. Abdeslem, and H. Ramdane, "Trajectory tracking performance with two nonlinear controllers of quadrotor under wind effect," in *2020 4th International Conference on Advanced Systems and Emergent Technologies (ICASET)*, Dec. 2020, pp. 50–55, doi: 10.1109/IC49463.2020.9318319.
- [29] MathWorks, "Dryden wind turbulence model (discrete)." MathWorks. <https://www.mathworks.com/help/aeroblks/drydenwindturbulencemodel-discrete.html> (Accessed on 27 May. 2022).

BIOGRAPHIES OF AUTHORS







Dounia Meradi     was born in Bordj Bou Arreridj, Algeria in 1992. She received the Engineer degree in Automatic and Control systems from the National Polytechnic School of Algiers (ENP). She is currently a Ph.D. candidate at the Laboratory of Signal Processing and Imaging (LATS), Saad Dahlab University in Blida. Her research interests are including optimal control, modeling, and nonlinear control of UAV. She can be contacted at email: dounia.meradi@g.enp.edu.dz.



Zoubir Abdeslem Benselama     is in the academic field for the last 30 years. He received the Engineer degree in 1985, from the Ecole Nationale Polytechnique d'Alger, Algiers, Algeria, the Master degree in 1997, from the Ecole Nationale Polytechnique d'Alger, Algiers, Algeria, and the Ph.D. degree in 2007 from the Ecole Nationale Polytechnique d'Alger, Algiers, Algeria, all in electrical engineering. Currently he is Professor at the Department of Electronics of the University of Blida, Blida, Algeria. His present interests are in Machine Learning and control process. He can be contacted at email: benselamaabd@hotmail.com.



Ramdane Hedjar     received the B.Sc. and Ph.D. degrees from the University of Science and Technology Houari Boumediene, Algiers, Algeria, in 1988 and 2002, respectively, and the MSc degree from the University of Blida in Algeria in 1992 in electronic and electrical engineering. After obtaining the PhD degree, he joined the Computer Engineering Department at King Saud University as an assistant professor. From 1992-2000, he was a lecturer with the Electronics Department at Djelfa University, and from 1994-2000 he was a research assistant with the Electronic Department at the University of Blida. Currently, he is a professor at King Saud University. His research interests include robust control, nonlinear predictive control, robotics, neural network control, and networked control systems. He can be contacted at email: hedjar@ksu.edu.sa.